Available online at www.sciencedirect.com

SCIENCE DIRECT®

Thin Solid Films 482 (2005) 264–269

thin solid films

www.elsevier.com/locate/tsf

PECVD a-C:H films for STW resonant devices

G. Cicala[a,*], P. Bruno[a], A. Dragone[b], A.M. Losacco[c], C. Sadun[d], A. Generosi[e]

[a]*Istituto di Metodologie Inorganiche e dei Plasmi (IMIP-CNR) Sezione di Bari Via G. Amendola 122/D 70126 Bari, Italy*
[b]*Dipartimento di Ingegneria Elettrotecnica ed Elettronica Politecnico di Bari, via Orabona 4, 70126 Bari, Italy*
[c]*Centro Laser, S.P. Casamassima km 3 70010 Valenzano (Bari), Italy*
[d]*Dipartimento di Chimica Universita' di Roma "La Sapienza" P.le Aldo Moro 5, Roma, Italy*
[e]*Istituto di Struttura della Materia (ISM-CNR) Via del Fosso del Cavaliere 100, 00133 Roma, Italy*

Available online 29 December 2004

Abstract

Plasma polymeric hydrogenated amorphous carbon (a-C:H) coatings have been found to be a promising material for use in surface transverse acoustic wave (STW) resonator employed as humidity sensor. The tailoring of coating properties has been easily obtained by variation of CH_4 percentage in CH_4–Ar mixture that enables to tune the response of polymer-coated STW resonator. Specifically, the optimum sensing characteristics of the STW resonator has been exhibited by coating obtained at 50% of CH_4 percentage. The correlation between the device sensitivity and the material properties, as determined by small angle X-ray scattering (SAXS), X-ray reflectivity (XRR), ellipsometry and Fourier infrared spectroscopy (FTIR) measurements, permits us to highlight the sensing mechanism of the active a-C:H coatings. The porosity has been considered the main effect on the enhancement of the sensor response.

Keywords: PECVD; Polymeric a-C:H films; STW device; Humidity sensor

1. Introduction

Abundant literature exists on several and different kinds of humidity sensors based on the measurements of the change of a particular physical parameter. The present paper deals with a novel humidity sensor based on a plasmapolymer-coated surface transverse acoustic wave (STW) resonant device that relies on a mass change of polymer coating upon the exposure to the relative humidity.

In these last years the micro/nanoporous materials such as porous silicon [1] and polymers [2–7] have attracted a lot of interest owing to their potential application in humidity sensor. In our earlier paper [5], polymeric coatings (such as hexamethyldisiloxane, HMDSO, and a-C:H) have been employed and tested on STW resonator. HMDSO film has been already utilized and its sensitivity has been linked to the higher oxygen in the polymer (i.e. to its hydrophilicity) [3], whereas polymeric a-C:H film has been used for the first time and it has been shown that this material is appropriate for humidity sensing.

Amorphous carbon films, produced by radio frequency Plasma Enhanced Chemical Vapor Deposition (r.f. PECVD) technique, have been widely and deeply investigated ([8] and refs. therein). It is well known that their amorphous matrix is a three-dimensional network composed of trigonally and tetragonally coordinated carbon atoms and voids ([9] and refs. therein). Specifically, the porous structure of polymer-like hydrogenated amorphous carbon (a-C:H) films is due to the low growth temperature (RT) that (a) promotes the high incorporation of hydrogen and (b) inhibits the mobility of adsorbed species at the surface as well as in its bulk leading to the void formation. The porosity extent also depends on the deposition rate of the film, at higher deposition rate indeed the growth precursors stick to the film surface where they land and do not have time to rearrange before the arrival of other species. Therefore, the void amount depends on the process parameters. Obviously, the porous structure limits the

* Corresponding author. Tel.: +39 080 592 9518; fax: +39 080 592 9520.
E-mail address: grazia.cicala@ba.imip.cnr.it (G. Cicala).

0040-6090/$ - see front matter © 2004 Elsevier B.V. All rights reserved.
doi:10.1016/j.tsf.2004.11.156

applications of polymeric a-C:H films as protective coatings, but they are of great technological importance for adsorption and hetereogeneous catalysis and in the present paper we propose and exploit them as active coating for STW resonator. The polymeric a-C:H can be thought as relatively open material that enables the permeation of gas such as water vapor into the film bulk. Specifically, the PECVD technique enables to tune the a-C:H film properties (e.g. micro/nanoporosity, density, refractive index, hydrogen content, structural and optical properties) by changing the CH_4 percentage in the CH_4–Ar mixture. The results of sensitivity measurements are complemented by small angle X-ray scattering (SAXS), X-ray reflectivity (XRR), ellipsometry and Fourier infrared spectroscopy (FTIR) ones reflecting the porosity, the density, the refractive index and the composition of the film, respectively. The correlation between the device sensitivity and the coating properties is discussed and allows to clarify and explain the sensing mechanism of the active a-C:H films.

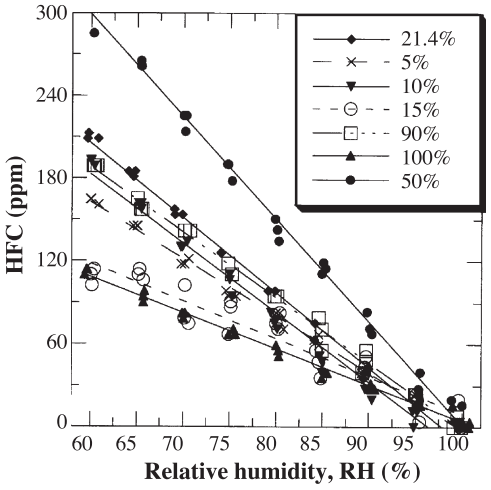

Fig. 1. Humidity frequency characteristics, HFC, for various polymeric a-C:H (obtained at different CH_4 percentages in the feeding CH_4–Ar mixture) coated-STW resonators as a function of relative humidity.

2. Experimental

2.1. Coating deposition

Polymer-like a-C:H coatings were produced from CH_4–Ar plasmas at 13.56 MHz in a conventional parallel plate PECVD reactor capacitively coupled to an r.f. supplier (ENI-Model ACG-5 generator). The substrates (crystalline silicon and AT-cut quartz) were placed onto the anode (grounded electrode) where the ion bombardment at the substrate during film growth can be neglected [10] (for the low developed plasma sheath voltage that guarantees the polymer-like character of carbon films). The depositions were carried out by keeping constant: growth temperature (25 °C, RT), total pressure (39.9 Pa), r.f. power (250 W), total flow rate, Φ_T, (70 sccm) and by changing the CH_4 percentage ($\%CH_4=\phi_{CH_4}/(\phi_{CH_4}+\phi_{Ar})\times 100$) of feeding CH_4–Ar mixtures in the range 5–100%. The thicknesses of the coatings were measured by a surface profiler (KLA-TENCOR® P-10) and were kept almost constant about 400 nm by varying the deposition time.

The sensing characteristics of the humidity sensor were determined on the AT-cut quartz substrates on which the STW resonant device was realized. The water vapor adsorption on a-C:H coatings was monitored measuring the shift in the resonance frequency. The STW operation principle was described in detail elsewhere [5]. The humidity frequency characteristics (HFC) were measured by a HP 8714ET Network Analyzer in a climatic chamber (Mazzali Climatest C330G5). The HFCs for samples obtained at various CH_4 percentages are plotted as a function of relative humidity in Fig. 1. The sensitivity changes for the various samples, and all the responses exhibit a good linearity.

The film properties were measured on the silicon substrates. The refractive index was obtained by means of a single-wavelength rotating compensated ellipsometer (SWE SOFIE Jobin Yvon) (He–Ne laser 0.5 mW, 632.8 nm, angle of incidence 70°).

Fourier Transform Infrared (FTIR NICOLET IMPACT 400 D) spectrophotometer was employed to measure the infrared transmission of a-C:H films and to estimate the hydrogen content incorporated in it. The number of C—H bonds (N_{C-H}) was evaluated by the following equation $N_{C-H}=A\int(\alpha(\omega)/\omega)d\omega$ where the integral is the area of the peak centered at about 2900 cm^{-1} (due to different CH_x (x=1–3) stretching vibrations), $\alpha(\omega)$ is the absorption coefficient dependent on the wavenumber and A (a normalization factor proportional to the inverse of the absorption strength) is about 2×10^{20} cm^{-2} for polymeric a-C:H films as reported by Jacob and Unger [11].

2.2. SAXS experiments

Reflection-mode small angle X-ray scattering (SAXS) experiments were carried out at the Chemistry Department of the University of Rome 'La Sapienza' by using an energy dispersive home-made X-ray diffraction (EDXD) apparatus elsewhere described [12,13]. Briefly, an incident polychromatic X-ray radiation is used and the scattered beam is energy resolved by a solid state detector located at a suitable scattering angle. The X-ray source is a standard Seifert tube operating at 50 kV and 40 mA whose Bremsstrahlung radiation is used; whereas the detecting system is composed of an EG&G liquid–nitrogen-cooled ultrapure Ge solid-state detector connected to a PC through ADCAM hardware.

The diffractometer operates in vertical θ/θ geometry and is equipped with an X-ray generator (tungsten, W, target), a collimating system, stepping motors, and a solid-state detector connected via an electronic chain to a multichannel analyzer. Both the X-ray tube and the detector can rotate

around their common center where the sample was placed. After a preliminary set of measurements, one scattering angle, θ=0.15° was selected to investigate the interesting range of the reciprocal space. The uncertainty associated to θ is $\Delta\theta$=0.001° and it affects directly the uncertainty Δq associated to the transfer momentum q defined as:

$$q = \text{const} \times E \times \sin\theta \quad (1)$$

where const=1.01354 $Å^{-1}$ keV^{-1}, E is the radiation energy (keV) and θ is the incidence angle (°). Typical SAXS scattering spectra are given in Fig. 2 in which the results of SAXS measurements are plotted versus the scattering vector q. The a-C:H films obtained at various CH_4 percentages show distinct profiles and intensities. The increase of SAXS intensity is indicative of a higher amount of pores in the material [14].

2.3. XRR experiments

The energy dispersive X-ray reflectometer (XRR) used is a non-commercial machine [15]. The instrument is provided with two benches, one carrying the X-ray tube, the other the energy sensitive detector, pivoting around a single central axis. The X-ray optical path is defined by four variable slits mounted on the arms. The arms are moved by two linear actuators driven by stepping motors and the tangent of the angle is read by two linear encoders. Both the minimum step movement and the resolution of the encoders are of 1 μm, which, in our case, permits a reproducible minimum angle increment of 0.004°.

XRR spectra, like SAXS ones, were collected by scanning a polychromatic X-ray beam. The advantages of the energy dispersive reflectometer on the angular dispersive counterpart, are the immobility of the experimental set-up and the high q resolution (approaching 10^{-4} $Å^{-1}$). Moreover, the stationarity of the experimental set-up reduces the systematic errors induced by the angular scan (misalignments and aberrations) and guarantees the reproducibility of the experimental conditions (particularly critical at small angles) when many consecutive measurements have to be performed, as in the present case.

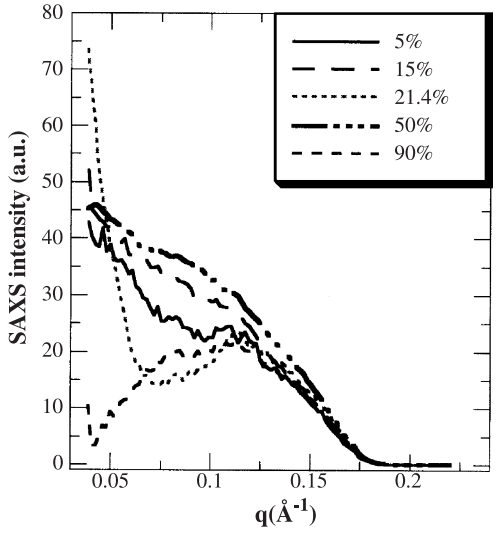

Fig. 2. Small angle X-ray scattering (SAXS) spectra from polymeric a-C:H films (deposited on silicon substrate and obtained at different CH_4 percentages in the feeding CH_4–Ar mixture) versus the scattering q vector.

An experimental scattering angle (θ) of 0.085° was fixed and the series of samples was measured under the same acquisition conditions (photon flux, energy, collimation slits, counting rates) to determine the position of their reflectivity edge. Once the reflectivity spectra were collected, the edges were fitted by a sigmoidal (Boltzmanian) curve to estimate the q_c (the critical q parameter) value. The q_c parameter is expressed by the following approximate formula:

$$q_c = \frac{\theta_c}{\lambda} = \left(\frac{Z\rho r_0}{2}\right)^{1/2} = \text{const} \quad (2)$$

where θ_c is the critical angle (defined by the condition for total external reflection), λ is the incident wavelength, ρ is the material density, r_0 is the classical electron radius and Z is the atomic number.

Both the position of the critical edge (q_c) and the slope of the reflectivity profile are determined by the material density. Typical XRR spectra are reported in Fig. 3a for bare and a-C:H coated Si substrate. In the XRR spectrum of Si substrate the critical edge is located at $q_{c\ Si}$=0.0307 $Å^{-1}$ ($\theta_{c\ Si}$=0.20°) using CuK_β radiation (λ=1.13926 Å) in Eq. (1). The $q_{c\ Si}$ value was used as a parameter to determine the accuracy of the measurements, and good agreement was found with literature [16]. In a-C:H coated Si substrates, the films change the shape of $q_{c\ Si}$, or induce two edges one related to the crystalline Si substrate ($q_{c\ Si}$) and the other to the deposited layer ($q_{c\ a\text{-}C:H}$). Particulars of XRR spectra of Fig. 3a, for the two films obtained at 10 and 50% of CH_4 percentage, are shown in Fig. 3b where the double critical q is clearly observed and localized at 0.0256 and 0.0242 $Å^{-1}$, respectively. The a-C:H film produced at 50% of CH_4, having the lowest value of $q_{c\ a\text{-}C:H}$, is the least dense.

Finally, no morphological information, such as thickness, can be deduced in these XRR spectra at higher value of q_c since no constructive interference fringes are visible. This may be due to the high value of thickness (400 nm), usually the XRR is used to measure thickness below 100 nm [16].

3. Results and discussion

Fig. 4 shows the deposition rate of polymeric a-C:H film grown on the grounded electrode (V_g=0) and the self-bias voltage, V_{bias}, recorded on the r.f. powered electrode [17]. By varying the CH_4 percentage, the trend of the deposition

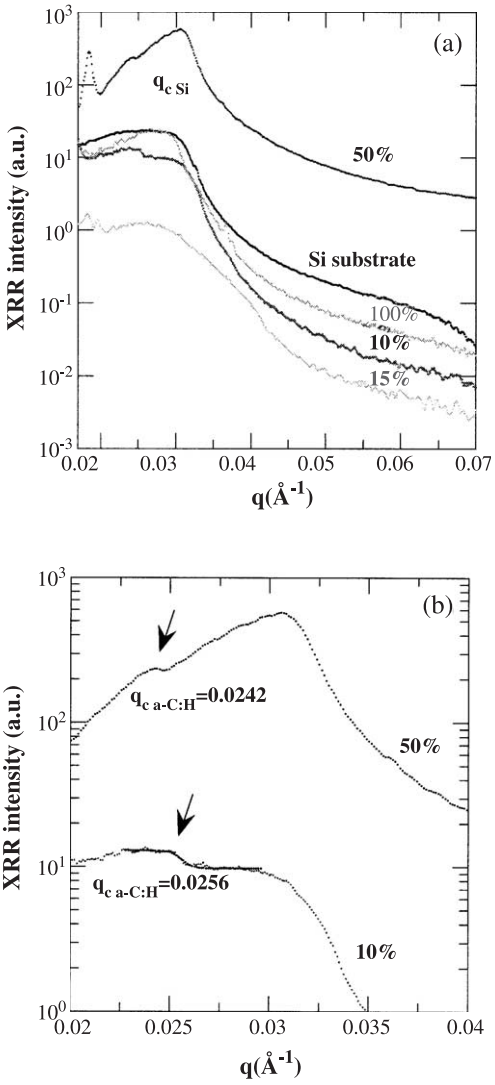

Fig. 3. (a) X-ray reflectivity (XRR) spectra from Si substrate and a-C:H films deposited on silicon substrate and obtained at different CH_4 percentages versus the scattering q vector; (b) particulars of XRR spectra of (a) for films obtained at 10 and 50% of CH_4 percentages to evidence better the distinct double critical q ($q_{c\ a\text{-}C:H}$) parameter.

rate of a-C:H films is akin to that of self-bias voltage that in turn is representative of the variation of plasma potential. Both curves r_D and V_{bias} have a maximum at 21.4%.

The relative frequency shift of polymeric a-C:H coated-STW resonator normalized to that of uncoated one is reported versus the CH_4 percentage in Fig. 5. The highest sensitivity is found for a-C:H coating obtained at intermediate values (50%) of CH_4 percentage.

Fig. 6 displays the values obtained by calculating the area under each SAXS curve of Fig. 2 as a function of CH_4 percentage. These values are used for a semiquantitative determination of the material porosity. The curve indicates that the more porous a-C:H film is produced at 50% of CH_4 percentage.

Fig. 7 shows the dependence of refractive index (n) and the hydrogen content (c_H) on the CH_4 percentage. The H

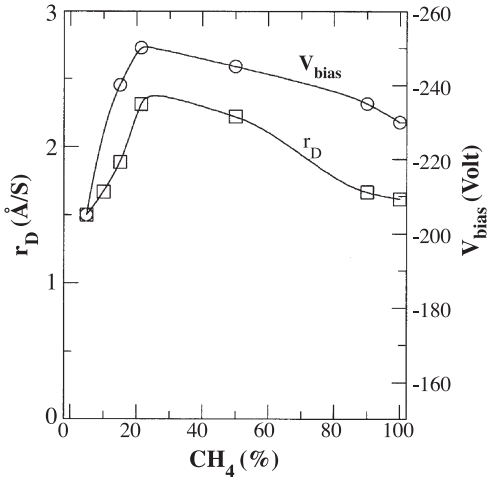

Fig. 4. Dependence of self-bias voltage (V_{bias}) and of deposition rate (r_D of the polymeric a-C:H films) on CH_4 percentage in the feeding CH_4–Ar mixture.

content in the film increases with increasing the CH_4 percentage, whereas the refractive index goes through a minimum localized at 50% of CH_4. Additionally, the lowest n corresponds to the lowest critical q parameter ($q_{c\ a\text{-}C:H}$=0.0242 $Å^{-1}$) well distinguishable in the least dense polymeric a-C:H film (reported in Fig. 3b). This result confirms the expected dependence between the refractive index (n) and the density of the film according to the following approximate equation [18]:

$$n^2 - 1 = \frac{4\pi N e^2 \hbar^2}{m E_g^2} \tag{3}$$

where the density of the material enters through N the density of valence-band electrons per unit volume, m and e

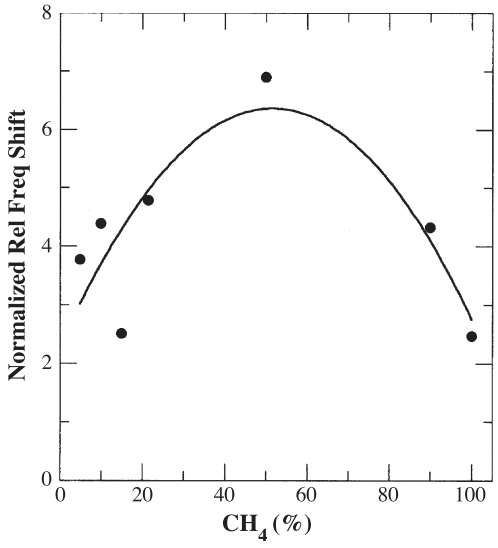

Fig. 5. Normalized relative frequency shift of polymeric a-C:H film coated-STW resonator as a function of CH_4 percentage, at constant relative humidity of 60%.

are electron mass and charge, $\hbar$ is the Planck's constant and E_g is the energy gap. Nevertheless, the lowest refractive index and density do not correspond to the highest hydrogen incorporation (Fig. 7) as usually reported in literature [18], in fact, in these materials the density dependence on H content is very small as already found by Ferrari et al. [16] in a wider range of c_H variation (c_H=10–50 at.%).

The change of mass of polymeric a-C:H films used as active coating on exposure to a water vapor is the sensing mechanism in a coated-STW resonator. Soft films such as polymer-like a-C:H because of their porosity are easily penetrated by water vapor. The water vapor adsorption/desorption processes on these kinds of film depend not only on the material porosity but also on the hydrophobicity and morphology of film surface. The knowledge of physical properties and composition of the film, as illustrated in Figs. 1–7, is very helpful in gaining information and in establishing what property favours the water vapor adsorption. The high hydrogen content (35–55 at.%), the low refractive index (1.5–1.6), the porous structure and the transparency confirm the polymeric nature of the a-C:H films [8]. The monotonous increase of c_H (Fig. 7) is explained on the basis of the continuous increase of CH_4, source of hydrogen; whereas the profile of the sensitivity (Fig. 5) seems to follow that of porosity (Fig. 6) and the deposition rate (Fig. 4) (even though with a slight shift of the maximum for this last). The variation of sensing characteristics of a-C:H coated-STW resonator as a function of CH_4 percentage could not be explained uniquely on the basis of H content but mainly of the void percentage. The H incorporation enhances the softness, but at the same time confers a hydrophobic character to the coating; thus, the presence of micro/nanopores is crucial in promoting the adsorption process. The microporous structure of a-C:H is determined by SAXS measurements (Figs. 2 and 6) and by optical micrograph (not reported). In particular, the a-C:H obtained

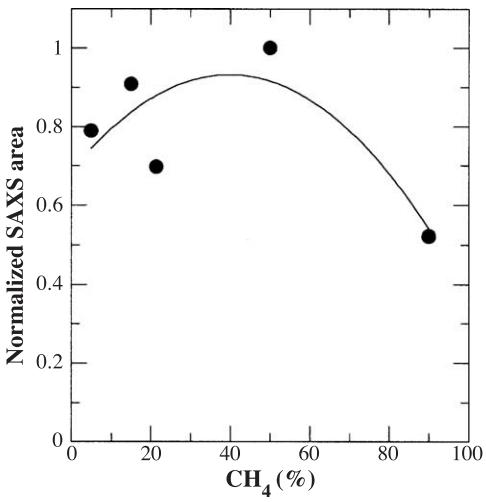

Fig. 6. Normalized area values of SAXS curves of the polymeric a-C:H films vs. CH_4 percentage in the feeding CH_4–Ar mixture.

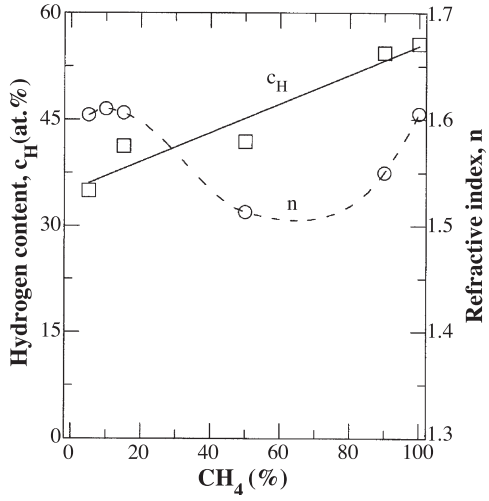

Fig. 7. Refractive index, n and hydrogen content, c_H (from FTIR spectra of the polymeric a-C:H films) vs. CH_4 percentage in the feeding CH_4–Ar mixture.

at 50% of CH_4 shows a network that contains interconnected pores, whereas films produced outside of this value are more compact. Finally, the combination of characterization methods enables to explain why the sensitivity curve shows a maximum at intermediate values of CH_4 percentage. The maximum is certainly due to the high concentration of pores or better to the presence of interconnected pores in the material network. The decrease of sensitivity at values of CH_4 percentage higher and lower than 50%, is ascribed to the more compact material. However, the sensitivity decrease, at CH_4 percentage higher than 50%, is also caused by the higher H content (Fig. 7) that makes more hydrophobic the surface and therefore inhibits the adsorption of water vapor. For the same reasons the minimum of refractive index curve (Fig. 7) and the lowest density of material (Fig. 3b) are easily justified.

4. Conclusions

The CH_4–Ar mixture fed PECVD reactor is utilized for the deposition of polymer-like a-C:H films on STW resonator employed as humidity sensor. The Ar addition to CH_4 gas is a useful approach for preparing polymeric a-C:H film having a variable micro/nanoporosity and H content. These films have been found to be good humidity sensing coatings for STW resonant device. HFC measurements of STW resonator in high relative humidity range (60–100%) has shown that the most active a-C:H coating is the least dense ($q_{c\ a\text{-}C:H}$=0.0242 $Å^{-1}$, n=1.5) and the most porous polymeric film, obtained at 50% of CH_4 percentage.

In light of these results, the porosity seems to be a key characteristic that enhances the response of the sensors and we can state that *the higher the porosity, the higher the sensitivity*. Further work is in progress to investigate the stability of the device response.

References

[1] Z.M. Rittersma, A. Splinter, A. Bodecker, W. Benecke, Sens. Actuators, B, Chem. 68 (2000) 210.
[2] F. Kraus, S. Cruz, J. Muller, Sens. Actuators, B, Chem. 88 (2003) 300.
[3] E. Radeva, L. Spassov, Vacuum 51 (1998) 217.
[4] E.I. Radeva, I.D. Avramov, Mater. Sci. Eng., C 12 (2000) 71.
[5] P. Bruno, G. Cicala, F. Corsi, A. Dragone, A.M. Losacco, Sens. Actuators, B, Chem. 100 (2004) 126.
[6] M. Bruzzi, S. Miglio, M. Scaringella, G. Bongiorno, P. Piseri, A. Podestà, P. Milani, Sens. Actuators, B, Chem. 100 (2004) 173.
[7] S. Belhousse, H. Cheraga, N. Gabouze, R. Outamzabet, Sens. Actuators, B, Chem. 100 (2004) 250.
[8] J. Robertson, Mater. Sci. Eng., R 37 (2002) 129.
[9] J.C. Angus, P. Koidl, S. Domitz, in: J. Mort, F. Jansen (Eds.), Plasma Deposited Thin Films, CRC Press, 1986, p. 89, Chap. 4.
[10] G. Cicala, G. Bruno, P. Capezzuto, in: H.S. Nalwa (Ed.), Handbook of Surfaces and Interfaces of Materials, Surface and Interface Phenomena, vol. I, Academic Press, San Diego, 2001, p. 509, Chap. 9.
[11] W. Jacob, M. Unger, Appl. Phys. Lett. 68 (1996) 475.
[12] V. Rossi Albertini, L. Bencivenni, R. Caminiti, F. Cilloco, C.J. Sadun, Macromol. Sci. Phys. 835 (1996) 199.
[13] R. Caminiti, V. Rossi Albertini, Int. Rev. Phys. Chem. 182 (1999) 263.
[14] L.G. Jacobsohn, G. Capote, M.E.H. Maia da Costa, D.F. Franceschini, F.I. Freire Jr., Diamond Relat. Mater. 11 (2002) 1946.
[15] V. Rossi Albertini, A. Generosi, B. Paci, P. Perfetti, G. Rossi, A. Capobianchi, A.M. Paoletti, R. Caminiti, Appl. Phys. Lett. 82 (2003) 3868.
[16] A.C. Ferrari, Surf. Coat. Technol. 180–181 (2004) 190.
[17] G. Cicala, P. Bruno, A.M. Losacco, G. Mattei, Surf. Coat. Technol. 180–181 (2004) 222.
[18] E.C. Freeman, W. Paul, Phys. Rev., B 20 (1979) 716.